Clays and Clay Minerals, Vol. 45, No. 5, 761–768, 1997.

CHARACTERIZATION OF THE SOLIDS OBTAINED BY PILLARING OF GRIFFITHITE (HIGH IRON CONTENT SAPONITE) WITH Al-OLIGOMERS

MIGUEL ANGEL VICENTE,[1] MERCEDES SUAREZ,[2] MIGUEL ANGEL BAÑARES–MUÑOZ[1] AND JOSE MARTIN–POZAS[2]

[1] Departamento de Química Inorgánica, Facultad de Química, Universidad de Salamanca, Plaza de la Merced S/N, 37008-Salamanca, Spain

[2] Area de Mineralogía y Cristalografía, Departamento de Geología, Facultad de Ciencias, Universidad de Salamanca, Plaza de la Merced S/N, 37008-Salamanca, Spain

Abstract—Griffithite, a high Fe content saponite (Griffith Park, California) was pillared with Al polymeric solutions, using different Al/clay ratios. The cation exchange began when Al-polycation solutions were added, being completed during the dialysis of the samples. Pillared solids were obtained by calcination of intercalated precursors at 500 °C. The content of Al_2O_3 increased from 7.35% in the natural griffithite to about 14% in the pillared samples, equivalent to the fixation of about 1.4 mmol Al per g of clay. The surface areas of the pillared griffithite were between 230–300 $m^2\ g^{-1}$. The intercalation and pillaring of griffithite were easier than that of a less-crystalline nonferrous saponite.

Key Words—Al_{13}-Keggin Polycation, Griffithite, Iron-Saponite, Pillaring, Porosity, Saponite.

INTRODUCTION

Intercalation of layered clays by bulk inorganic polycations and calcination of the intercalated precursors yield porous solids with regular porosity and a high number of acid sites. Polycations of different elements, such as Al, Zr, Ga, Cr or Ti, have been used. Montmorillonite is the most common layered silicate and it has been the most used in pillaring studies. The pillared solids improve the thermal stability of natural clays and have good catalytic properties (Figueras 1988; Occelli 1988).

Saponite, a magnesic smectite, is a product of the hydrothermal alteration and weathering of basalts and ultramafic rocks. This mineral is much less common than the aluminous smectite montmorillonite. Saponite is mainly tetrahedrally charged. Its octahedral sites are occupied by Mg(II) cations, but in its ferrous variety Fe(II,III) they substitute Mg(II) octahedral cations; this substitution is important when the ratio Mg/Fe is lower than 5:1 (De la Calle and Suquet 1988).

Although montmorillonite is the preferred clay mineral used in pillaring studies (Lahav et al. 1978; Figueras et al. 1990; Fetter et al. 1994; Ge et al. 1994; Kloprogge et al. 1994; Lahodny-Sarc and Khalaf 1994; Mokaya and Jones 1994; Storaro et al. 1995), saponite has also been intensely studied in the recent years. Both natural saponites (Usami et al. 1992; Chevalier et al. 1992; Chevalier, Franck, Suquet et al. 1994; Chevalier, Franck, Lambert et al. 1994; Schoondheydt et al. 1992, 1993, 1994; Li et al. 1993; Malla and Komarneni 1993; Lambert et al. 1994; Suquet et al. 1994; Bergaoui, Lambert, Suquet and Che 1995) and synthetic saponites (Bergaoui, Lambert, Franck et al. 1995; Bergaoui, Lambert, Vicente–Rodríguez et al. 1995) have been used in these studies, and new data about the mechanism of pillaring process have been obtained. Applicability of pillared saponite as catalysts (Usami et al. 1992; Chevalier, Franck, Lambert et al. 1994; Suquet et al. 1994) and in metal retention (Bergaoui, Lambert, Suquet and Che 1995) has been investigated.

Griffithite (Griffith Park, California) is a high Fe content saponite with a ratio Mg:Fe of 1.85. The acid activation of this clay has been recently reported (Vicente Rodríguez et al. 1994, 1995). In the present study, it was intercalated with Al oligomers. The pillared solids were obtained by calcination of intercalated precursors at 500 °C. At the same time, a nonferrous saponite from Yunclillos (Toledo, Spain) was also pillared. The pillaring process and the textural properties of the solids obtained by pillaring of both saponites were compared.

EXPERIMENTAL

Pillaring of Saponite

Griffithite was obtained by aqueous decantation of the <2 μm fraction of the basaltic rock from Griffith Park deposit (California, supplied by Minerals Unlimited, Ridgecrest, California). The structural formula of the <2 μm sample was found to be: $[Si_{6.92}\ Al_{1.08}]\ O_{20}\ (OH)_4\ [Mg_{2.92}\ Fe_{1.58}\ Al_{0.28}\ Ti_{0.04}\ Mn_{0.06}]\ [Ca_{0.62}Na_{0.20}K_{0.04}]$ and its cation exchange capacity (CEC) was 0.86 meq/g (Vicente Rodríguez et al. 1994, 1995).

Griffithite was intercalated with Al oligomeric solutions, obtained by hydrolysis of $AlCl_3{\cdot}6H_2O$ with

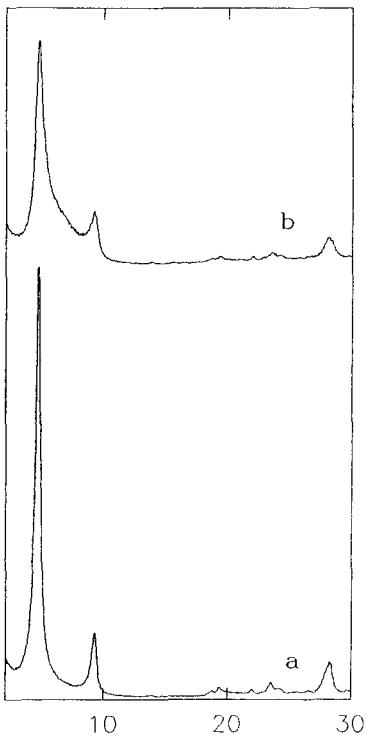

Figure 1. XRD patterns of samples before (b) and after (a) dialysis in griffithite 7.5 series.

NaOH. The ratio OH^-/Al^{3+} was 2.2 and the volume of the pillaring solutions was 450 mL. Under these conditions, most of Al polymerizes to $[Al_{13}O_4(OH)_{24}(H_2O)_{12}]^{7+}$, a polycation designated as Keggin ion or Al_{13}, but other Al species also exist in solution (Fu et al. 1991). These solutions were maintained at room temperature for 24 h and added to previously prepared suspensions of 6 g of the clay in 550 mL of water, followed by stirring for 24 h. Ratios of 2.5, 5.0 and 7.5 mmol Al per g of clay were used. The samples were then centrifuged and washed by dialysis until chloride-free. Then they were centrifuged and dried at 60 °C, giving the intercalated solids (designated as IS2.5GR, IS5.0GR and IS7.5GR; the numbers refer to the Al/clay ratios). Calcination at 500 °C for 4 h, with a heating rate of 1 °C min^{-1} from room temperature up to 500 °C, gave the pillared compounds (designated as PS2.5GR, PS5.0GR and PS7.5GR).

The <2 μm fraction of the nonferrous saponite from Yunclillos deposit (Toledo, Spain, supplied by TOLSA, Madrid) was also obtained by aqueous decantation. The structural formula of this sample is $[Si_{7.42}Al_{0.58}]O_{20}(OH)_4[Mg_{5.16}Fe_{0.14}Al_{0.26}Ti_{0.018}Mn_{0.004}][Mg_{0.24}Ca_{0.124}Na_{0.020}K_{0.084}]$, and its CEC is 1.15 meq/g (Vicente et al. 1996). This sample was intercalated with Al oligomer solutions following the described procedures and using a 2.5 mmol Al per g of clay ratio (IS2.5YU sample). Pillared Yunclillos saponite (PS2.5YU sample) was obtained by calcination of the intercalated solid in the same conditions as described for griffithite.

Techniques

Elemental analyses were carried out by plasma emission spectroscopy, using a Perkin–Elmer emission spectrometer, model Plasma II. Previously, the solids were digested under pressure, in a nitric–hydrofluoric acid mixture, in a polytetrafluoroethylene (PTFE) autoclave. X-ray diffractograms were obtained on a Siemens D-500 diffractometer at 40 kV and 30 mA (1200 W) with filtered Cu$K\alpha$ line. The equipment is connected to a DACO-MP microprocessor and uses Diffract-AT software. For obtaining X-ray diffraction (XRD) patterns before and after dialysis, a few drops were taken from the suspensions and oriented films were prepared. Intercalated and pillared solids were studied by the powder method. Fourier transform infrared (FTIR) spectra were obtained in the region 4000–350 cm^{-1} on a Perkin–Elmer 1730 FTIR spectrometer, equipped with a 3700 data station, by the KBr pellet technique. Specific surface areas were determined from the corresponding nitrogen isotherms at 77 K, obtained from a Micromeritics ASAP 2010 analyzer, after outgassing the samples at 110 °C for 8 h to a residual pressure of 10^{-5} mm Hg. The Brunauer–Emmett–Teller (BET) method was used for the calculations.

RESULTS AND DISCUSSION

The intercalation and pillaring processes were studied by XRD at 4 different stages: 1) after addition of Al_{13} solution and stirring for 24 h (studied as oriented film); 2) after dialysis (also studied as oriented film); 3) the intercalated solids; and 4) the pillared solids. The diffractograms show that the ion exchange process begins, in all cases, during the addition of Al_{13} solutions, and it is completed after the dialysis process (Figure 1). For griffithite, reflections at 18.66, 19.44 and 18.75 Å appear after addition of the Al_{13} solution (Table 1). These peaks have shoulders at lower spacings, thus proving that not all the sheets have been intercalated. In Yunclillos saponite, there is a broad peak centered at 16.95 Å, indicating that the ion exchange process is less complete than in griffithite. After dialysis, the basal spacings remain constant in griffithite (18.71, 19.07 and 18.91 Å), while in Yunclillos saponite, the spacing increases until 18.33 Å. The peaks are now narrower and more symmetric than before dialysis, indicating that the washing of the samples completes the intercalation process, as has been observed by other authors (Lahav et al. 1978; Figueras et al. 1990; Fetter et al. 1994).

The intercalated and pillared compounds show similar XRD patterns in all the series considered (Figure 2). In griffithite, the basal spacings of intercalated solids is about 18.8 Å, which corresponds to the inter-

https://doi.org/10.1346/CCMN.1997.0450514 Published online by Cambridge University Press

Table 1. Basal spacings of 001 reflection of oriented films and powder samples and FWHM index of 001 reflection peak for powder samples.

Sample	Basal spacing (Å)	FWHM (°2θ)
BD2.5GR	18.66	
AD2.5GR	18.71	
IS2.5GR	18.70	0.576
PS2.5GR	17.42	0.673
BD5.0GR	19.44	
AD5.0GR	19.07	
IS5.0GR	18.87	0.531
PS5.0GR	17.58	0.617
BD7.5GR	18.75	
AD7.5GR	18.91	
IS7.5GR	18.89	0.523
PS7.5GR	17.73	0.646
BD2.5YU	16.95	
AD2.5YU	18.33	
IS2.5YU	18.07	1.345
PS2.5YU	17.43	1.525

Key: BD = oriented film before dialysis; AD = oriented film after dialysis; IS = intercalated solids; PS = pillared solids; GR = griffithite; YU = Yunclillos saponite.

calation of Al_{13} polycations with their major axis perpendicular to the layers of the clay. The value decreases in pillared solids to about 17.6 Å after calcination at 500 °C. In Yunclillos saponite, the intercalated sample has a basal spacing of 18.1 Å, decreasing to 17.4 Å in the pillared sample. The full widths at half maximum (FWHM index), given in Table 1, indicate that well-ordered intercalation compounds are obtained, the solids obtained by treatment of griffithite being more crystalline than those obtained from Yunclillos saponite. For the pillared compounds, the intensity of the $d(001)$ peak is similar in the 3 series. In Table 2 the 001, 002, 004 and 006 spacings of intercalated and pillared samples are given. The product (Bragg l index × Basal spacings) indicates that samples have good crystallinity, the greater deviations corresponding to 006 reflection. The crystallinity is similar in the 3 series considered and better for intercalated than for pillared samples.

The FTIR spectra of natural and intercalated saponite are displayed in Figure 3. Only small differences are observed between the raw and the intercalated saponite, differences that confirm the intercalation process. At 3616 cm^{-1}, a band is clearly observed in intercalated solids while it appeared only as a shoulder in griffithite, this band being assigned to Al-O-H stretch. The band at 519 cm^{-1}, corresponding to the Si-O-Al mode, increases with intercalation, being especially significant in the sample intercalated with 2.5 mmol Al per g of clay, while in natural griffithite it appears only as a shoulder. At 920 cm^{-1}, a shoulder due to (Mg,Al)-OH bonds can be observed in the intercalated solids (Kloprogge et al. 1994). These modes are more intense in the intercalated than in the natural

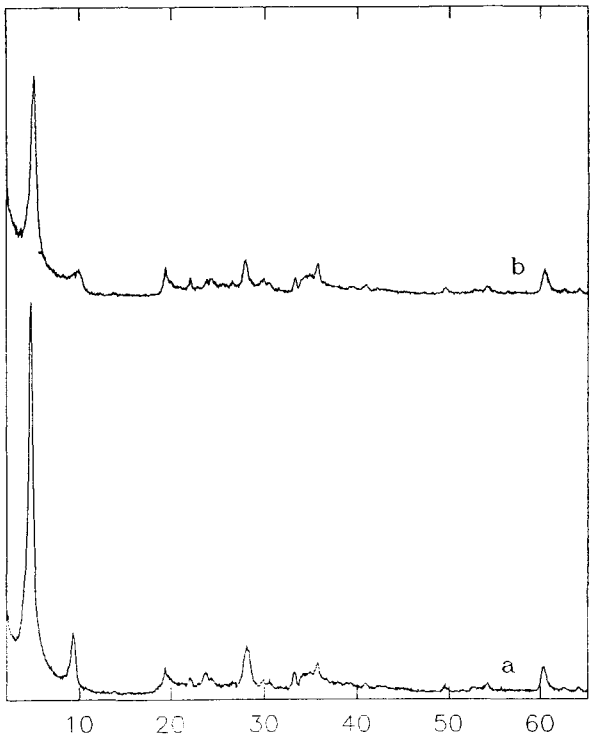

Figure 2. XRD patterns of samples intercalated (a) and pillared (b) in griffithite 2.5 series.

griffithite; the differences between the natural and the intercalated samples can be clearly observed because of the low content of Al in the natural sample. At the same time, the band corresponding to Fe-OH bonds, which appears at 584 cm^{-1} in raw griffithite, is not observed in the intercalated solids.

The Al content in natural and intercalated solids is given in Table 3 and increases in intercalated griffithite by about 7% with respect to the raw material. The percent increases correspond to the fixation of about 1.4 mmol Al per g of clay. This amount is very similar in all samples and independent of the concentration of Al in the intercalating solutions. In Yunclillos saponite, a 6.93% increase in Al_2O_3 content is observed in

Table 2. The 001, 002, 004 and 006 spacings of intercalated and pillared samples.

Sample	$d(001)$ (Å)	$d(002)$ (Å)	$d(004)$ (Å)	$d(006)$ (Å)
IS2.5GR	18.70	9.47	4.57	3.17
PS2.5GR	17.42	8.97	4.56	3.20
IS5.0GR	18.87	9.47	4.59	3.17
PS5.0GR	17.58	8.95	4.55	3.19
IS7.5GR	18.89	9.49	4.59	3.19
PS7.5GR	17.73	8.97	4.58	3.20
IS2.5YU	18.07	†	4.53	3.20
PS2.5YU	17.43	†	4.52	3.16

† Masked by a mica peak at 9.9 Å.

https://doi.org/10.1346/CCMN.1997.0450514 Published online by Cambridge University Press

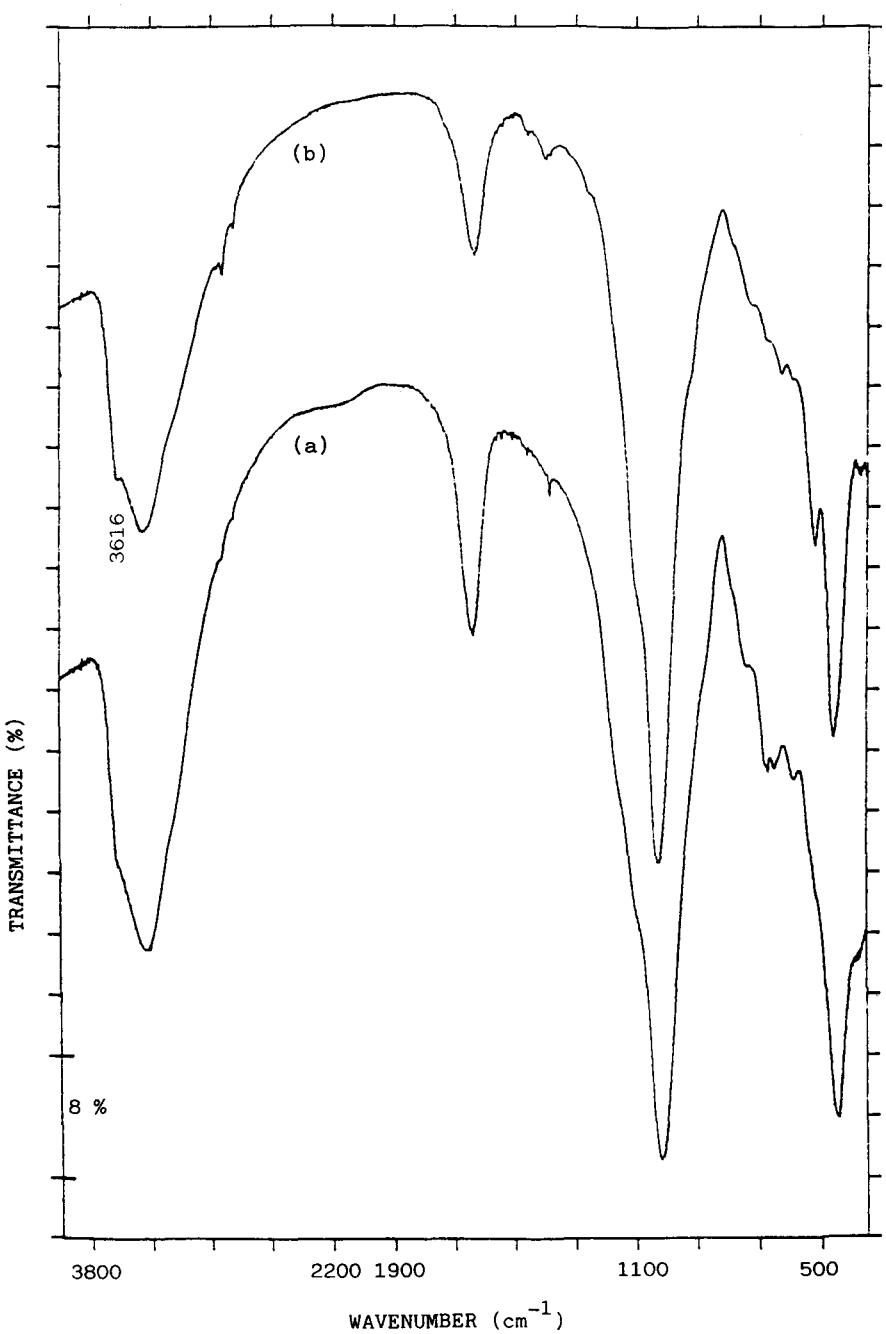

Figure 3. FTIR spectra of raw (a) and 2.5 mmol Al per g intercalated (b) griffithite.

intercalated sample with respect to the natural one. The concentration of the pillaring solutions is in the range usually reported for pillaring of montmorillonite and saponite in the literature, in which solutions from as diluted as 1.8 mmol Al per g of clay (Ge et al. 1994) or 2 mmol Al per g of clay (Lahodny-Sarc and Khalaf 1994) to very concentrated solutions (Schoondheydt et al. 1992, 1993, 1994) have been used.

Specific surface areas of both intercalated and pillared solids were determined from their nitrogen isotherms by using the BET method; data are given in Table 4. The surface area of intercalated griffithite is about 300 $m^2\ g^{-1}$, while in Yunclillos saponite the intercalated solid has a surface area of 221 $m^2\ g^{-1}$. In pillared griffithite, the surface area decreases by about 20%, except for the sample PS7.5GR, whose area is

https://doi.org/10.1346/CCMN.1997.0450514 Published online by Cambridge University Press

Table 3. Si and Al content (wt% in oxides) of natural and pillared samples.

Sample	SiO_2	Al_2O_3	Al_2O_3†
Griffithite	44.02	7.35	7.35
IS2.5GR	38.08	14.14	16.34
IS5.0GR	39.12	14.17	15.94
IS7.5GR	41.61	13.93	14.74
Yunclillos saponite	52.90	4.35	4.35
IS2.5YU	46.03	11.28	12.96

† Referred to SiO_2 content in natural saponites (44.02% in griffithite and 52.90% in Yunclillos saponite).

Table 4. BET surface area of natural, intercalated and pillared griffithite and Yunclillos saponite.

Sample	S_{BET} ($m^2\ g^{-1}$)
Griffithite	35
IS2.5GR	306
PS2.5GR	255
IS5.0GR	299
PS5.0GR	233
IS7.5GR	294
PS7.5GR	293
Yunclillos saponite	161
IS2.5PU	221
PS2.5PU	201

practically constant with respect to the intercalated sample, having a high surface area of 293 $m^2\ g^{-1}$. In Yunclillos saponite, the pillared sample has a low surface area, 201 $m^2\ g^{-1}$, with a decrease of only 10% with respect to the intercalated sample and only slightly higher than that of natural sample, 161 $m^2\ g^{-1}$. It must be considered that natural Yunclillos saponite has a surface area higher than that usually reported for natural saponites, probably due to the sedimentary origin of the Madrid Basin, in which the Yunclillos deposit is located.

Surface areas of 425 and 403 $m^2\ g^{-1}$ have been reported for Ballarat saponite intercalated and pillared at 500 °C, respectively (Chevalier, Franck, Lambert et al. 1994; Suquet et al. 1994). Malla and Komarneni (1993) have also pillared this sample, and found a surface area of 320 $m^2\ g^{-1}$ when calcining at 500 °C. Schoonheydt et al. (1993, 1994) have reported surface areas between 214 and 247 $m^2\ g^{-1}$ when pillaring saponite with different OH/Al ratios and calcining at 550 °C. When studying the intercalation and pillaring of variable charge layer Fe-free synthetic saponites (7.5 mmol Al per g of clay), Bergaoui, Lambert, Suquet and Che (1995) and Bergaoui, Lambert, Franck et al. (1995) have found values between 360 and 457 $m^2\ g^{-1}$ for intercalated solids and between 280 and 417 $m^2\ g^{-1}$ for pillared (500 °C) samples. The surface area of pillared griffithite is similar to that reported for nonferrous pillared natural saponites but lower than that reported for synthetic saponites, while the surface area of intercalated and pillared Yunclillos saponite is lower than that found in other saponites, but similar to that reported by Schoonheydt et al. (1993, 1994).

The surface area of the pillared solids seems to be related to the crystallinity of original samples and to the origin of their layer charge. The influence of the layer charge has been reported in the literature. Kloprogge et al. (1994) have observed that when the negative charge in the layer is originated from Si-Al substitutions in the tetrahedral sheets, the existence of Si-OH-Al groups favors the pillaring process. Plee et al. (1987), studying the pillaring of beidellite and montmorillonite, have observed a more ordered distribution of pillars in the clays rich in tetrahedral substitutions. We can now compare the behavior of 2 saponites with differences in crystallinity and in the origin of the layer charge. Griffithite is much more crystalline that Yunclillos saponite, a difference that is maintained in the corresponding intercalated and pillared samples, as was indicated when discussing the results of Table 1. Natural griffithite is a very well-crystallized sample and its charge is mainly originated by tetrahedral Si-Al substitutions, while in Yunclillos saponite, less crystalline than griffithite, the layer charge is more related to octahedral holes. These 2 effects justify the better pillaring ability observed in griffithite.

The porosity of the different solids was studied by numerical analyses of their nitrogen isotherms. A computer program was used (Rives 1991), mainly employing the "*t*" (Lippens and de Boer 1965) and "*f*" (Cranston and Inkley 1957) methods. The microporosity in griffithite samples decreases from intercalated to pillared solids, as shown by the extrapolation of *t* plots (Figure 4). The same behavior is observed in Yunclillos saponite. The pore size distributions, obtained from the adsorption branch of the nitrogen isotherms, are similar for the different solids. The pore distributions of all the pillared solids are given in Figure 5. A sig-

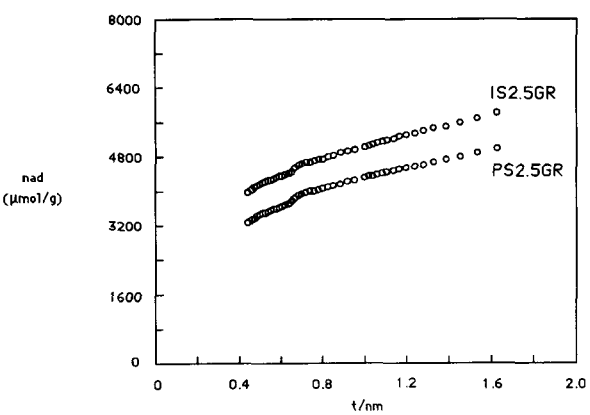

Figure 4. A *t* plot of intercalated and pillared griffithite in 2.5 series.

https://doi.org/10.1346/CCMN.1997.0450514 Published online by Cambridge University Press

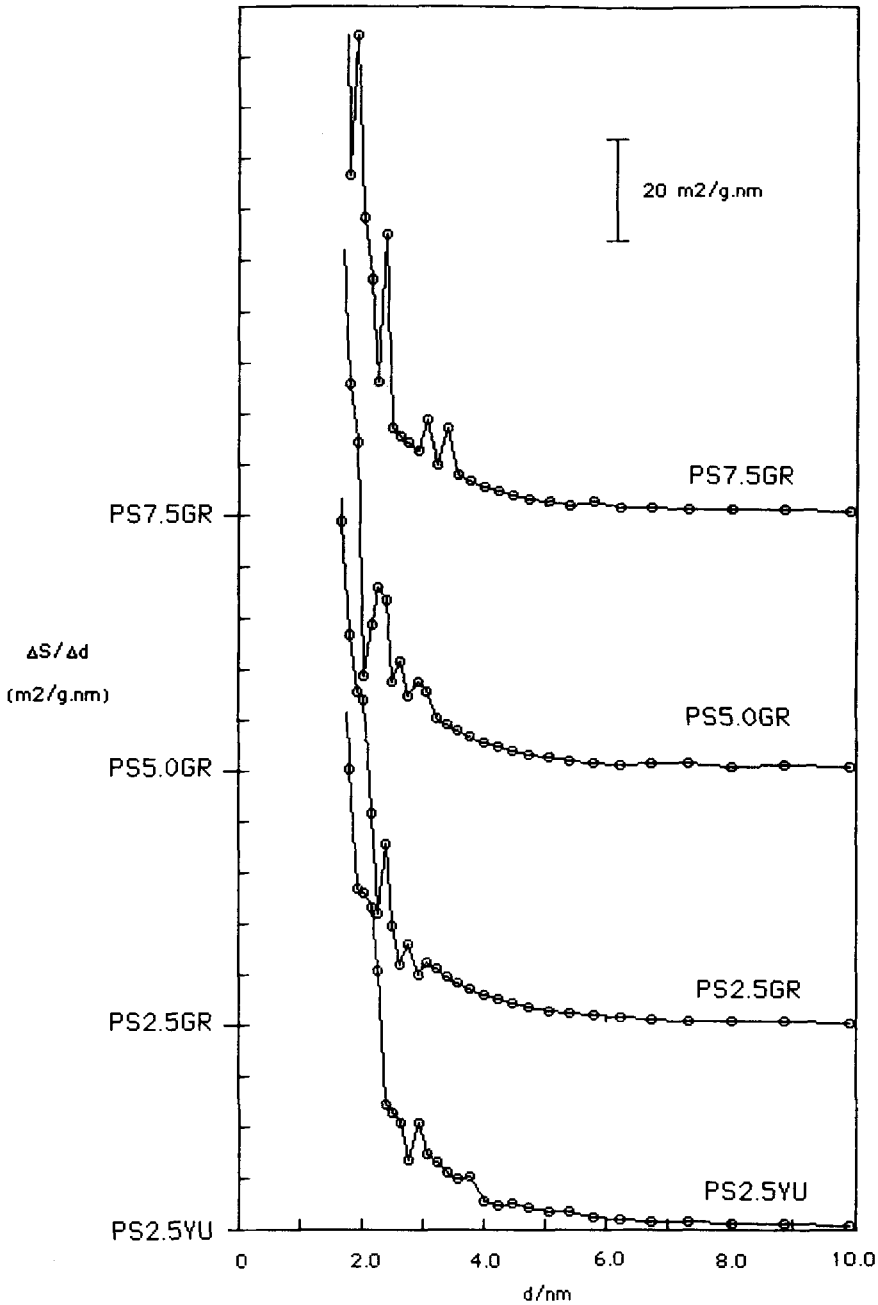

Figure 5. Pore size distribution of pillared griffithite (the "zero" of each representation is indicated in the vertical axis).

nificant fraction of pores is found in the micropore region and all samples show an important amount of pores between 20–40 Å in diameter, the sample PS7.5GR, that has the largest surface area, has also the largest porosity.

The comparison of the nitrogen adsorption process is made by using the f plot. A similar behavior is observed for all samples in the entire relative pressure range. Thus, if the adsorption in pillared samples is studied using the intercalated samples as reference, a parallel line at $f \approx 0.8$ is observed, the lower amount of nitrogen adsorbed by the pillaring sample being the only difference in the adsorption process. In series 7.5, the adsorption process is very similar, both in form and in amount, before and after calcination, in agreement with the maintenance of surface area. When comparing the adsorption process of the intercalated solid corresponding to each of the 3 series, no signif-

https://doi.org/10.1346/CCMN.1997.0450514 Published online by Cambridge University Press

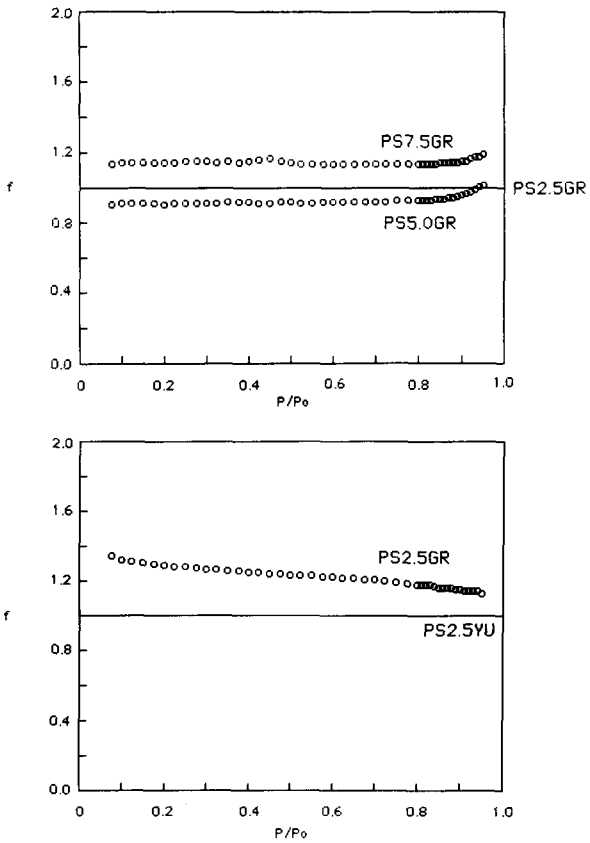

Figure 6. a) An *f* plot of pillared griffithite, the sample PS2.5GR being the reference. b) An *f* plot of 2.5 pillared griffithite compared to 2.5 pillared Yunclillos saponite (reference).

icant differences were observed; the same behavior was observed when the 3 pillared solids were compared (Figure 6a), the higher amount of nitrogen adsorbed by the sample PS2.5GR being the only difference. When comparing pillared griffithite with pillared Yunclillos saponite, the higher amount of nitrogen adsorbed by griffithite was observed, the main difference being in the region of low pressure (Figure 6b), that is, in the region corresponding to microporosity, in agreement with the porosity indicated by the pore size distributions.

CONCLUSIONS

Griffithite, a high Fe content saponite, has a great ability to form intercalation compounds with Al polymeric species. The cation exchange process begins during the addition of Al solution and it is completed during the washing dialysis of the solids.

The obtained solids fix a high amount of Al (about 6.7% of Al_2O_3). The larger fixation of Al is obtained when a relation of 2.5 mmol Al per g of clay is used, the smaller ratio employed. The surface area of the solids obtained is about 300 $m^2\ g^{-1}$ for intercalated solids and decreases approximately 20% when calcining, except for 7.5 series, in which the pillared sample has a surface area of 293 $m^2\ g^{-1}$. The intercalation and pillaring ability of griffithite is higher than that observed in Yunclillos saponite. The crystallinity of natural sample (higher in griffithite) and the origin of the layer charge (tetrahedral in griffithite and octahedral in Yunclillos saponite) justify this better ability of griffithite to form intercalated and pillared solids. No significant differences in the porosity or in the texture are observed when comparing the intercalated and pillared griffithite with the solids obtained from the intercalation and pillaring of the nonferrous Yunclillos saponite.

ACKNOWLEDGMENT

Financial support of Comisión Interministerial de Ciencia y Tecnología, CICYT, (MAT 96-0643 Project) is gratefully acknowledged.

REFERENCES

Bergaoui L, Lambert JF, Franck R, Suquet H, Robert JL. 1995. Al-pillared saponites. Part 3. Effect of parent clay layer charge on the intercalation-pillaring mechanism and structural properties. J Chem Soc, Faraday Trans 91:2229–2239.

Bergaoui L, Lambert JF, Suquet H, Che M. 1995. Cu^{II} on Al_{13}-pillared saponites: Macroscopic adsorption measurements and EPR spectra. J Phys Chem 99:2155–2161.

Bergaoui L, Lambert JF, Vicente-Rodríguez MA, Michot LJ, Villiéras F. 1995. Porosity of synthetic saponites with variable layer charge pillared by Al_{13} polycations. Langmuir 11:2849–2852.

Chevalier S, Franck R, Lambert JF, Barthomeuf D, Suquet H. 1992. Stability of Al-pillared saponites: Evidence of disorganization during storage in air. Clay Miner 27:245–248.

Chevalier S, Franck R, Lambert JF, Barthomeuf D, Suquet H. 1994. Characterization of the porous structure and cracking activity of Al-pillared saponites. Appl Catal A: General 110:153–165.

Chevalier S, Franck R, Suquet H, Lambert JF, Barthomeuf D. 1994. Al-pillared saponites. Part 1. IR studies. J Chem Soc, Faraday Trans 90:667–674.

Cranston RW, Inkley FA. 1957. The determination of pore structures from nitrogen adsorption isotherms. Adv Catal 9:143–154.

De la Calle C, Suquet H. 1988. Vermiculite. Rev Mineral 19. In: Bailey SW, editor. Hydrous phyllosilicates. Washington, DC: Mineral Soc Am. p 455–496.

Fetter G, Tichit D, Massiani P, Dutarte R, Figueras F. 1994. Preparation and characterization of montmorillonites pillared by cationic silicon species. Clays Clay Miner 42:161–169.

Figueras F. 1988. Pillared clays as catalysts. Catal Rev Sci Eng 30:457–499.

Figueras F, Klapyta Z, Massiani P, Mountassir Z, Tichit D, Fajula F, Gueguen C, Bosquet J, Auroux A. 1990. Use of competitive ion exchange for intercalation of montmorillonite with hydroxy-aluminum species. Clays Clay Miner 38:257–264.

Fu G, Nazar LF, Bain AD. 1991. Aging processes of alumina sol-gels: Characterization of new aluminum polyoxocations by aluminum-27 NMR spectroscopy. Chem Mater 3:602–610.

Ge Z, Li D, Pinnavaia TJ. 1994. Preparation of alumina-pillared montmorillonites with high thermal stability, regular microporosity and Lewis/Brönsted acidity. Microporous Mater 3:165–175.

Kloprogge JT, Boy E, Jansen JBH, Geus JW. 1994. The effect of thermal treatment on the properties of hydroxy-Al and hydroxy-Ga pillared montmorillonite and beidellite. Clay Miner 29:153–167.

Lahav N, Shani U, Shabtai J. 1978. Cross-linked smectites. I. Synthesis and properties of hydroxy-aluminum-montmorillonite. Clays Clay Miner 26:107–115.

Lahodny–Sarc O, Khalaf H. 1994. Some considerations of the influence of source clay material and synthesis conditions on the properties of Al-pillared clays. Appl Clay Sci 8:405–415.

Lambert JF, Chevalier S, Franck R, Suquet H, Barthomeuf D. 1994. Al-pillared saponites. Part 2. NMR studies. J Chem Soc, Faraday Trans 90:675–682.

Li L, Liu X, Ge Y, Xu R, Rocha J, Klinowski J. 1993. Structural studies of pillared saponite. J Phys Chem 97:10389–10393.

Lippens BC, de Boer JH. 1965. Studies on pore systems in catalysis. V. The *t* method. J Catal 4:319–323.

Malla PB, Komarneni S. 1993. Properties and characterization of Al_2O_3 and SiO_2-TiO_2 pillared saponite. Clays Clay Miner 41:472–483.

Mokaya R, Jones W. 1994. Pillared acid-activated clay catalysts. J Chem Soc Chem Commun 1994:929–930.

Occelli ML. 1988. Physicochemical properties of pillared clay catalysts. Stud Surf Sci Catal 35. In: Kaliaguine S, editor. Keynotes in energy-related catalysis. Amsterdam: Elsevier. p 101–137.

Plee D, Gatineau L, Fripiat JJ. 1987. Pillaring processes of smectites with and without tetrahedral substitution. Clays Clay Miner 35:81–88.

Rives V. 1991. A computer program for analyzing nitrogen adsorption isotherms on porous solids. Adsorption Sci Tech 8:95–104.

Schoonheydt RA, van den Eynde J, Tubbax H, Leeman H, Stuyckens M, Lenotte I, Stone WEE. 1993. The Al pillaring of clays. Part I. Pillaring with dilute and concentrated Al solutions. Clays Clay Miner 41:598–607.

Schoonheydt RA, Leeman H. 1992. Pillaring of saponite in concentrated medium. Clay Miner 27:249–252.

Schoonheydt RA, Leeman H, Scorpion A, Lenotte I, Grobet P. 1994. The Al pillaring of clays. Part II. Pillaring with $[Al_{13}O_4\ (OH)_{24}\ (H_2O)_{12}]^{7+}$. Clays Clay Miner 42:518–525.

Storaro L, Ganzerla R, Lenarda M, Zanoni R. 1995. Vapour phase deep oxidation of chlorinated hydrocarbons catalyzed by pillared bentonites. J Mol Catal A: Chemical 97:139–143.

Suquet H, Franck R, Lambert JF, Elsass F, Marcilly C, Chevalier S. 1994. Catalytic properties of two pre-cracking matrices; a leached vermiculite and a Al-pillared saponite. Appl Clay Sci 8:349–364.

Usami H, Tagaki K, Sawaki Y. 1992. Regioselective photocyclodimerization of cyclohexenones intercalated on clay layers. Chem Lett 1992:1405–1408.

Vicente Rodríguez MA, López González JD, Bañares-Muñoz MA. 1995. Preparation of microporous solids by acid treatment of a saponite. Microporous Mater 4:251–264.

Vicente Rodríguez MA, Suárez Barrios M, López González JD, Bañares-Muñoz MA. 1994. Acid activation of a ferrous saponite (Griffithite): Physico-chemical characterization and surface area of the products obtained. Clays Clay Miner 42:724–730.

Vicente MA, Suárez M, López González JD, Bañares-Muñoz MA. 1996. Characterization, surface area, and porosity analyses of the solids obtained by acid leaching of a saponite. Langmuir 12:566–572.

(Received 8 August 1996; accepted 27 January 1997; Ms. 2812)